JOURNAL OF AIRCRAFT
Vol. 41, No. 4, July–August 2004

Iterative Inverse Design Method Based on Streamline Equations

Jianzhong Yu* and Ion Paraschivoiu†
École Polytechnique de Montréal, Montréal, Québec H3C 3A7, Canada
and
Farooq Saeed‡
King Fahd University of Petroleum and Minerals, Dhahran 31261, Saudi Arabia

Aerodynamic characteristics are very sensitive to airfoil leading-edge geometry, and its accurate treatment is a limitation of many existing design methods. The objective of the present research is to develop an interactive inverse design method that is not only efficient but can also treat the leading-edge region accurately. In the formulation of the method, a small-perturbation geometric equation is deduced from the streamline momentum equations, the continuity equation, and the isentropic relations with the geometry similarity assumption of near streamlines to the airfoil surface. Moreover, the transonic correction is considered in the aforementioned equation with the assumption for the effects of waves reflected from the free surface (sonic line) because the method based on the surface flow values cannot take into account the transonic characteristics such as wave interference. The geometric perturbation normal to the airfoil surface is then calculated by solving this second-order initial value ordinary differential equation iteratively to obtain an airfoil design. Techniques such as airfoil smoothing, nonuniform relaxation, and the strained coordinate transfer are employed to accelerate convergence. The airfoil design cases demonstrate the remarkable efficiency and accuracy of the method not only for compressible flows but also for low-speed flows. Moreover, the method allows the leading-edge shape to be determined accurately and, thus, to overcome the deficiency of many of the related methods.

Nomenclature

A	=	function defined by Eq. (11)
a	=	speed of sound, m/s
B	=	coefficient of the equation
C, D	=	constants
c	=	airfoil chord length
c_p	=	pressure coefficient
d	=	ordinary derivative
F, f	=	functions of Mach number and pressure coefficient
F'	=	$\partial F/\partial c_p$, Eq. (12)
M	=	Mach number
p	=	pressure
x, y	=	Cartesian coordinates
α	=	angle of attack
γ	=	specific heat ratio
Δ	=	increment
η	=	direction or coordinate normal to airfoil surface
ϑ	=	Prandtl–Meyer function or the angle between characteristic line and the streamline
κ	=	curvature
ρ	=	density
ω	=	angle between characteristic line and the airfoil surface

Subscripts

o	=	objective or target value
s	=	surface value
0	=	initial value
∞	=	freestream value

Received 17 August 2002; revision received 30 January 2004; accepted for publication 30 January 2004.

*Graduate Research Assistant, Département de Génie Mécanique, CP 6079, Succ. Centre-ville.
†Bombardier Aeronautical Chair Professor, Département de Génie Mécanique, CP 6079, Succ. Centre-ville. Associate Fellow AIAA.
‡Assistant Professor, Aerospace Engineering Department, Mail Box 1637. Member AIAA.

Introduction

THERE are numerous aerodynamic inverse design methods available for airfoil or wing design. Among these design methods, the iterative or iterative residual-correction methods such as Takanashi's[1] and NASA's streamline curvature method[2–5] are very powerful for engineering applications. They are based on iterative corrections of pressure or velocity differences between the target and designed airfoils and are only required to predict the correct geometric variation tendencies rather than the exact values as the solution will be improved during the iteration process. Moreover, the flow solver is retained in its original form and can be treated just like a "black box." Therefore they can be directly coupled with any newly developed and more efficient flow solver and can be easily applied to complicated configurations because of their flexibilities.

Inverse design methods also have inherent problems such as single-point design limitation and present difficulties in adding constraints. Moreover, the specified target pressure distribution cannot guarantee minimum drag. Furthermore, iterative inverse design methods are generally not very accurate, and their precision such as maximum tolerance or maximum pressure coefficient differences is rarely discussed. It is generally accepted, from a practical point of view, that if the graphical differences between the target and design pressure distributions are small enough the accuracy of the method is taken for granted because in this case the lift, drag, and moment differences between the two airfoils are so small that the design requirements can be met without any problem.

As a result of limitations of inverse design methods, efforts have to be made for geometry smoothing, for verification of aerodynamic performance at off-design conditions or incorporation of additional constraints, and for modification of target pressure distribution, which is often obtained in engineering design by modifying the pressure distribution of an existing airfoil whose certain characteristics are required to be preserved and others to be improved. Because aerodynamic characteristics are very sensitive to the leading-edge geometry as it plays a very important role in low-speed maximum lift, transonic shock location, etc., it is difficult to preserve the key aerodynamic characteristics of the original airfoil if the design method cannot work well in the leading-edge region. Therefore,

accurate calculation of airfoil shapes, especially leading-edge shapes, is essential for efficiency of inverse design methods.

Hence, most of the existing design methods do not perform very well in leading-edge regions owing to large flow gradients and high curvature distributions. As a result, their practical applications are limited because aerodynamic characteristics are very sensitive to airfoil leading-edge geometric shapes. More recently, several approaches have been tried to improve or overcome this limitation. Takanashi's streamline curvature method[2] is successfully employed for subsonic flows, but it is not very efficient in other flow regimes. Representation of airfoil geometry by families of smooth analytic functions[6,7] is an effective way, but the design results are restrictive. The objective of the current research under the Bombardier Aeronautical Chair at Ecole Polytechnique is to develop an iterative inverse method that is not only efficient but also accurate for both compressible and low-speed flows. The design method has been developed for use by the Advanced Aerodynamics Department of Bombardier Aerospace.

In this paper, a new iterative inverse design method based on streamline equations is presented. Instead of the typical assumptions to streamline curvature variations normal to the airfoil surface, as in the streamline curvature methods, a small perturbation geometric equation is deduced from the streamline momentum equations, the continuity equation, and the isentropic relations with the geometry similarity assumption of near streamlines to the airfoil surface. Moreover, the transonic correction is also considered in this equation with the assumption for the effects of waves reflected from the free boundary (sonic line) because the method based on the surface flow values cannot take into account the transonic characteristics like wave interference. For the specified target pressure distribution and the initial airfoil, the stagnation point is taken as the initial point with its zero perturbation value, and then the geometric perturbation normal to the airfoil surface can be calculated by solving this ordinary differential equation as initial-value problem. The airfoil is designed in iteration. Techniques such as airfoil smoothing, nonuniform relaxation and the strained coordinate, which are employed to remove nonuniformity from perturbation solutions of nonlinear problems, are applied for accelerating the convergence. The high efficiency and accuracy of this method is demonstrated by several subsonic and transonic airfoil design cases. In addition, some concerned problems are also discussed in detail.

Governing Equations

The momentum equation with the isentropic relations along a streamline can be written as

$$[\gamma/(\gamma-1)](p/\rho)+V^2/2=[\gamma/(\gamma-1)](p_\infty/\rho_\infty)+V_\infty^2/2 \quad (1)$$

The momentum equation normal to the streamline has the following form:

$$\rho V^2\kappa=\frac{\partial p}{\partial \eta} \quad (2)$$

For a streamline tube very near the airfoil surface, as shown in Fig. 1, with the first-order accuracy for η, the continuity equation can be approximated as

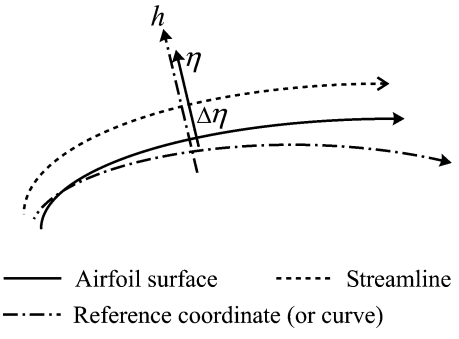

Fig. 1 Streamline tube and its coordinates near the airfoil.

$$\rho V\eta+\frac{1}{2}\frac{\partial(\rho V)}{\partial\eta}\eta^2=C \quad (3)$$

Assuming small differences between target and design airfoils, the following equations can be obtained:

$$(\rho V)_o=(\rho V)+\Delta(\rho V), \qquad \eta_o=\eta+\Delta\eta$$
$$\left[\frac{\partial(\rho V)}{\partial\eta}\right]_o=\left[\frac{\partial(\rho V)}{\partial\eta}\right]+\Delta\left[\frac{\partial(\rho V)}{\partial\eta}\right] \quad (4)$$

Substituting Eq. (4) into Eq. (3) gives

$$(\rho V)_o\Delta\eta+\eta\Delta(\rho V)+\eta\Delta\eta\frac{\partial(\rho V)}{\partial\eta}+\frac{1}{2}\eta^2\Delta\left[\frac{\partial(\rho V)}{\partial\eta}\right]$$
$$+\eta\Delta\eta\Delta\left[\frac{\partial(\rho V)}{\partial\eta}\right]=0 \quad (5)$$

Because the target pressure distribution is generally specified for inverse design, it is convenient to express the variables in Eq. (5) as functions of pressure coefficients along with the preceding equations and the following equation of state, Eq. (6), the speed of sound relation, Eq. (7), the isentropic relation, Eq. (8), and the definition of the pressure coefficient, Eq. (9), as follows:

$$p=\rho RT \quad (6)$$

$$a^2=\gamma RT \quad (7)$$

$$\left(\frac{p}{\rho}\right)^\gamma=\left(\frac{p_\infty}{\rho_\infty}\right)^\gamma \quad (8)$$

$$c_p=\frac{2(p-p_\infty)}{\rho_\infty V_\infty^2} \quad (9)$$

Thus the following dimensionless relations can be obtained:

$$F(c_p,M_\infty)=\rho V/\rho_\infty a_\infty=\sqrt{2}\left(1+\tfrac{1}{2}\gamma M_\infty^2 c_p\right)^{1/\gamma}A \quad (10)$$

where

$$A=\left[\tfrac{1}{2}M_\infty^2+1/(\gamma-1)-[1/(\gamma-1)]\left(1+\tfrac{1}{2}\gamma M_\infty^2 c_p\right)^{(\gamma-1)/\gamma}\right]^{\frac{1}{2}} \quad (11)$$

Consequently,

$$\frac{1}{\rho_\infty a_\infty}\frac{\partial(\rho V)}{\partial\eta}=-\frac{\partial F}{\partial c_p}\frac{\partial c_p}{\partial\eta}=F'f\kappa \quad (12)$$

where f is a function of c_p and M_∞ given by

$$f(c_p,M_\infty)=\left(4/M_\infty^2\right)\left(1+\tfrac{1}{2}\gamma M_\infty^2 c_p\right)^{1/\gamma}A^2 \quad (13)$$

Used together with Eqs. (10) and (12), Eq. (5) becomes

$$\eta F+\tfrac{1}{2}\eta^2\kappa F'f=0 \quad (14)$$

Replacing η, F, κ, and f in the preceding equation with $\eta+\Delta\eta$, $F+\Delta F$, $\kappa+\Delta\kappa$, and $f+\Delta f$, respectively, and ignoring higher-order terms of $\Delta\eta$, we obtain

$$\left(\tfrac{1}{2}\eta+\Delta\eta\right)\eta F'f\Delta\kappa+(F_o+\eta F_o'f_o\kappa)\Delta\eta+\eta\Delta F$$
$$+\tfrac{1}{2}\eta^2\kappa\Delta(F'f)=0 \quad (15)$$

From Eq. (4) and Fig. 1, we have

$$\eta_o=h_o-h_{\text{os}}, \qquad \eta_o=h-h_s$$

As a result,

$$\Delta\eta \approx (h - h_o) - (h_{os} - h_s) = \Delta h - \Delta h_s \tag{16}$$

where h is the coordinate normal to the reference curve (which can be considered as one of target and designed airfoil surfaces).

The streamlines very close to the airfoil surface are geometrically similar to the airfoil form itself, and there is almost no difference between streamlines very far from the airfoil because of the same freestream condition; therefore, it can be assumed that the difference between a near streamline around the target airfoil and the corresponding streamline around the designed airfoil is proportional to and smaller than that between the two airfoils. That is to say,

$$\Delta\eta = -D\Delta h_s \tag{17}$$

where D is a small positive constant and can be made equal to the initial streamline value of the design airfoil without loss of generality:

$$D = \eta_0/c \tag{18}$$

In addition, note that the curvature increment is given by

$$\Delta\kappa = \frac{\partial^2 \Delta h_s}{\partial s^2} \tag{19}$$

Thus, using Eqs. (14–19), the following equation can be deduced:

$$A_1 \frac{\partial^2 \Delta h_s}{\partial s^2} + A_3 \Delta h_s + B = 0 \tag{20}$$

where

$$A_1 = \left(\tfrac{1}{2}\eta + \Delta\eta\right)\eta F' f, \qquad A_3 = -\left(F_o + \eta F_o' f_o \kappa\right)(\eta_0/c)$$

$$B = \eta\Delta F + \tfrac{1}{2}\eta^2\kappa\Delta(F' f) \tag{21}$$

The preceding equation cannot be applied directly because of the following reasons. The ordinary differential equation, Eq. (20), is very stiff because the first coefficient A_1 is of the same order as the other coefficients near the leading edge, whereas away from which A_1 decreases very rapidly. But this term cannot be ignored even if it is made much smaller by choosing a smaller $\Delta\eta$. Otherwise it is impossible to get a reasonable solution near the leading edge because of its large curvature variations. Furthermore, applying Eq. (20) to the whole airfoil leads to nonphysical solutions because the ignored terms can be of the same order as the coefficient A_1 or even greater in the regions other than the leading edge. Thus physically it is meaningless to keep using this equation. Therefore for the remaining part of the airfoil the following algebraic equation is used, which is derived from Eq. (20) by ignoring the first term. Hence,

$$A_3 \Delta h_s + B = 0 \tag{22}$$

For transonic flow, it can be shown that $F' = \partial(\rho V)/\partial c_p$ dominates the properties of the first coefficient of Eq. (20) and is positive for supersonic flows, negative for subsonic flows, and null at the sonic point. That is to say, the sonic point is a singular point for Eq. (20). In fact, this singular point does not pose any serious problem because this term is much smaller than the others; hence, it can be ignored within the supersonic zone, and Eq. (22) used instead. Moreover, the term B of Eq. (22) dominated by the difference $\Delta F = \Delta(\rho V)$ also shows different tendencies for subsonic and supersonic flows. Hence with the same pressure difference, the direction of geometric perturbations for supersonic flows is opposite to that of subsonic flows. In addition, for supersonic flows the flow influence region is only limited in Mach zones, and as a result Eq. (22) should be adapted, and it is more suitable to solve the following differential form of Eq. (15), with the first term ignored and treated as an initial value problem:

$$A_{2T}\Delta\eta' + A_{3T}\Delta\eta + B_T = 0 \tag{23}$$

where

$$A_{2T} = F_o + \eta F_o' f_o \kappa, \qquad A_{3T} = F_o' c_{p,o}' + \eta' F_o' f_o \kappa$$

$$B_T = \eta\Delta(F' c_p') + \eta'\Delta F + \eta\eta'\kappa\Delta(F' f) \tag{24}$$

However, transonic flows with their small supersonic zones can be greatly different from pure supersonic ones with very far free boundaries. The supersonic variation relation between the geometry and the pressure is not valid everywhere for transonic flow, especially at the beginning of the small supersonic zone where the general geometry and pressure variations might still obey the subsonic relations. This phenomenon can be simply explained by reflection of expansion waves from the very near sonic line as shown by Farrari and Tricomi[8] or Moulden.[9] These reflected waves are compressive and tend to slow down the flow. Therefore if there is a small concave region even invisible on the airfoil surface, the flow can decelerate instead of accelerating because of the effects of reflected compressive waves and vice versa. Moreover, for transonic flows it is not appropriate to express the geometry similarity assumption of near streamlines to the airfoil surface as in Eq. (17), an additional relation of streamline slopes might be preferred. Furthermore, the preceding equations are based on the surface values rather than the whole flowfield. Therefore they cannot reflect transonic flow characteristics such as wave interference. The correction to transonic effects must be taken into account, which is realized by the treatments based on following ideas. Streamline slopes are the same along their isoclines, but only from the surface variables it is impossible to define the isoclines. Consequently, an approximated relation is obtained from characteristic lines whose direction is known at the airfoil surface because it is well known that the angle ϑ between the left characteristic line and the streamline satisfy the relation (Ref. 9, p. 110): $\vartheta + \omega = \text{constant}$.

It is assumed that the slope difference of near streamlines between the target and design airfoils is proportional to and smaller than that between the two airfoil forms along the characteristic lines, that is,

$$\Delta h_s' - \Delta h_c' = D\Delta h_s' \tag{25}$$

where D is a small positive constant and the subscript c represents the value at the characteristic line.

Because the equation will be solved as an initial value problem, the left characteristics are supposed to be dominant because they can directly affect the flow before a search point. Thus from the geometric relations, as shown in Fig. 2, and the Mach angle relation, we obtain

$$\eta' = h' - h_s' \approx h_c' + \frac{\partial h_c'}{\partial s}\Delta s - h_s', \qquad \Delta s \approx \eta\cot\vartheta = \sqrt{M^2 - 1}$$

$$\frac{\partial h_c'}{\partial s} \approx \frac{\partial h_s'}{\partial s} = \kappa \tag{26}$$

With similar relations used for Eq. (17) and with the higher-order terms ignored, the following approximated differential equation for

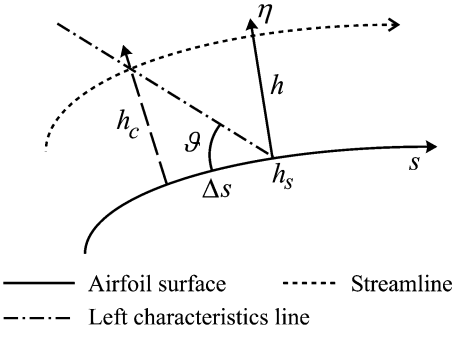

Fig. 2 Geometric relations between an airfoil surface, a near streamline and a left characteristic line from the airfoil.

transonic flows can be obtained:

$$C\Delta h_s' - \kappa\eta\left(\sqrt{M_o^2-1} - \sqrt{M^2-1}\right) - \kappa\Delta\eta\sqrt{M^2-1} + \Delta\eta' = 0 \tag{27}$$

The preceding equations are only applied for correction purposes. And thus they are only required to predict correct tendencies rather than exact values because solutions will be improved during the iteration process. Of course, the approximation precision will exert great influence on convergence speed, that is to say, on the efficiency of the method.

Perturbation Calculation and the Design Process

The geometry similarity assumption of near streamlines to the airfoil surface is not valid near the stagnation point where the geometric shape of even a very near streamline is greatly different from the airfoil shape. But the nearer the streamline line is to the airfoil surface, the smaller this invalid region is. Consequently it is appropriate to take the two discrete numerical points around the stagnation point of the design airfoil as the initial calculation points and then to calculate the perturbation before and after the stagnation point separately. This measure has been found to be effective because with the increase of iteration times the stagnation locations of the target and the design airfoils generally become so close and can be confined between the two initial points that the invalidity of the similarity assumption should not bring about any problem.

As the transonic design is the most complicated, the main procedure used for geometric perturbation calculation is as follows:

1) Calculate the near streamline coordinates η with the given initial value η_0 (1% airfoil chord generally used) with the help of Eq. (14).

2) Solve Eq. (20).

3) When a jump appears in the solution of Eq. (20) or the ratio of its first and second coefficients is smaller than a given value (1% is generally used), Eq. (22) is used instead.

4) From the first sonic point, Eqs. (23) and (27) are solved as the initial value problem.

5) After the shock position or the last sonic point, Eq. (20) is used again.

6) Perform a coordinate transfer to match the supersonic solution with the subsonic one after the shock, and keep it unchanged near the first sonic point during the first few iterations.

Step 6 can be looked as a correction measure to avoid shocks becoming stronger because the shocks on the airfoil tend to become stronger with each iteration because transonic flows are influenced by the presence of wave interferences and propagations and shocks are simply the envelops of compressive waves. The assumption that the left characteristics are dominant is mainly based on design and calculation experience and is used to attain convergence. It can, however, cause larger errors near strong shocks.

The principal airfoil design process, as shown in Fig. 3, is as follows:

1) Calculate the pressure distribution of the initial airfoil using a flow solver (viscous or nonviscous).

2) Perform the strained coordinate transfer for the target c_p distribution during the first few iterations. This is discussed more in a later section.

3) Calculate the normal geometric perturbation as just indicated.

4) Correct the calculated perturbations and perform the strained coordinate transfer for them if needed.

5) Apply a nonuniform relaxation to the small perturbation equation for convergence acceleration. This is also discussed more in a later section.

6) Add the geometric perturbation normal to the design airfoil.

7) Smooth the new airfoil.

8) Calculate the new leading-edge and trailing-edge locations, transfer them to original ones, or make the trailing-edge gap equal to the given one if specified.

9) Repeat the preceding steps until the convergence criterion is satisfied.

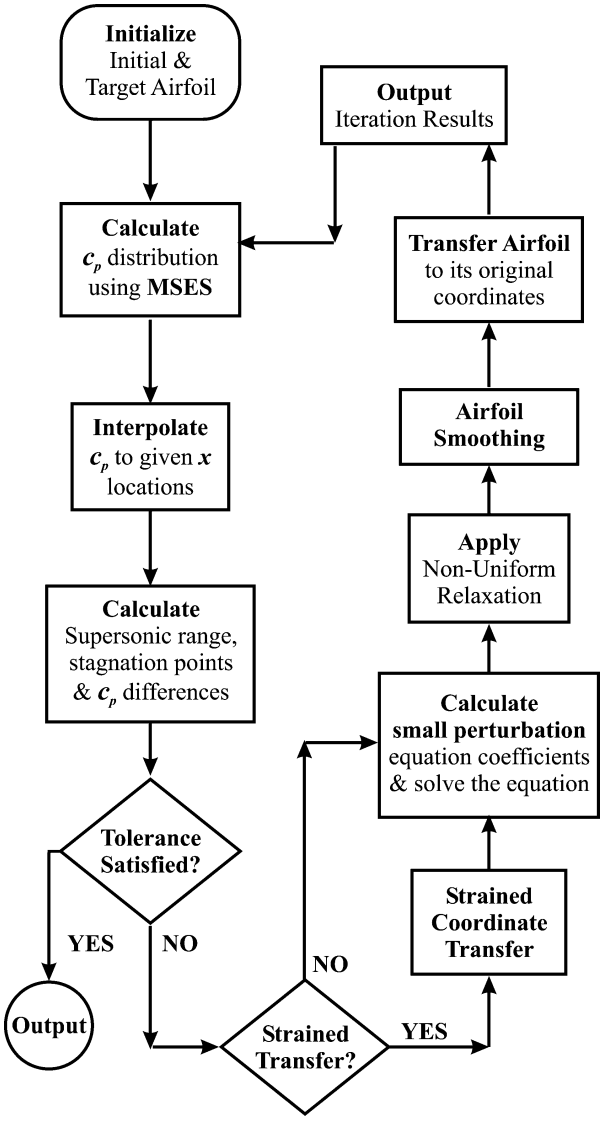

Fig. 3 Flowchart of the inverse design process.

Different convergence criteria are employed in design process. The principal one is that the maximum pressure coefficient difference between the target and the designed is smaller than 0.006. Even this value is not very small, but it is still so demanding that this kind of criterion has never been acceptable in any iterative correction method.[1–5] In fact, the precision of iterative inverse methods is generally judged from the graphical differences between the target and design pressure or velocity distributions, and its exact amplitude like the maximum pressure and geometric difference is rarely discussed. Exceptions can also exist, such as in the case of Milholen's paper,[2] in which a precision of ± 0.005 was specified for most cases and was numerically determined. In the present study, the solution is accepted at a specified iteration number if the graphical differences between the target and the designed pressure coefficients are small enough as the convergence criterion for the specified maximum pressure coefficient difference cannot always be satisfied.

Flow Solver: MSES

To compute the airfoil pressure distributions, the flow solver MSES[10–12] of Mark Drela, Massachusetts Institute of Technology, is employed. MSES is a multi-element airfoil design and analysis tool for a wide range of Mach and Reynolds numbers that includes low Reynolds numbers and transonic Mach numbers. For the purpose of the current study, only the analysis part of MSES was utilized. It has the capability to predict flows with transitional separation bubbles, shock waves, trailing edge, and shock-induced separation. It is also

able to predict surface pressure and aerodynamic forces accurately just past the stall.

The numerical formulation of MSES is based on a finite volume discretization of the steady Euler equations that make use of an intrinsic streamline grid. A two-equation integral formulation with lagged-dissipation closure is used to describe the boundary layers and trailing-edge wakes. The inviscid and viscous interaction regions are fully coupled through the displacement thickness. The airfoil surface is used to specify a solid-body boundary condition. The overall system is solved using a full Newton iteration method. The numerical accuracy of the MSES code has been established via comparison with known experimental data, and the reader is asked to refer to the associated references[10–12] for details. The code is being used widely in academia as well as industry.

Some Special Treatments

Strained Coordinate Transfer

Pressure differences between the target and calculated airfoils near the leading edge and the shock positions can be so large especially during the first few iterations that the calculated geometric perturbation can be greatly deformed because of the large differences between their stagnation points, suction peak, and the shock locations where the small perturbation assumption is not valid in this case. Geometry smoothing can help solve the problem, but the strained coordinate transfer can be more efficient.

The concept of employing coordinate straining to remove nonuniformities from perturbation solutions of nonlinear problems is well established. It was originally proposed by Lighthill[13] five decades ago and has found more applications[14–16] in the 1970s and 1980s, but to our knowledge the technique has not been applied to the treatment of airfoil geometries. The basic idea of this technique is that a straightforward perturbation solution might possess the right form, but not quite at the appropriate location.

There are two kinds of strained transfer used according to Stahara[14]: 1) in a "classical" sense, strained transfer is applied to full governing equations and boundary conditions. Thus, the differential equations so obtained are generally more complicated than the original ones, and 2) strained transfer is employed directly to the known nonuniform solution and then solving algebraic rather than differential equations. It is obvious that the second one is more suitable for the present design method based only on the known airfoil surface variables.

This technique was often used for nonlinear interpolation of two similar solutions. The coordinate transfer is carried out generally with the help of polynomials. The strained range and its vanishing manner should be carefully considered.[14] For the purpose of inverse design, the requirements for strained coordinate transfer are much more demanding in order to keep the geometric precision of the designed airfoil. Thus, in this research the transfer is applied only during the first few iterations for accelerating the convergence and a transfer based on Bezier spline is tried instead of polynomials for the sake of control flexibility. Moreover, the strained transfer is used for similar solutions, whereas the pressure distribution of the calculated airfoil during initial iterations might not be similar at all to the target. For example, one might have a suction peak near the leading edge and another might not. Therefore only some of the critical points such as leading edge, trailing edge, stagnation point, suction peak location, sonic point, and shock location of the two solutions need to be selected as strained points according to different situations. The application technique is similar to that as demonstrated in Ref. 16.

Airfoil Smoothing

Geometry smoothing is very important and even essential to some inverse methods for which the airfoil smoothing is used during each design iteration.[2] Because airfoil smoothing effects need to be meticulously controlled, it is impossible to directly apply the general method, which tends to smooth an airfoil too much or too less. Therefore, special methods suitable for airfoil smoothing must be developed.

In this study, several smoothing methods were adapted. The global smoothing technique is based on the optimized airfoil parameterization method.[17–19] This method can keep the third-order derivatives continuous, but its smoothing effects are very local because it is designed for accurately representing the original airfoil. Thus in shock regions, another smoothing method based on the original idea of Renz[20] is adapted. With this method, the second-order derivatives of perturbations are smoothed, and the differences between the smoothed derivatives and the original ones are integrated back to get the geometry difference. In addition, during the first few iterations the leading edge is smoothed with the sixth-order polynomial fitting if the maximum perturbation is larger than a specified value (say about 0.001). The Bezier function is widely used in the leading-edge region during the design process and has been found to be very efficient because it is able to preserve the general tendency of the original curve, damp the too high peaks, and keep the slope continuous at the two ends. If this kind of smoothing is not used, the calculation convergence is slower because of the oscillations and noises of the geometric perturbation solution in the leading-edge region.

Nonuniform Relaxation

In the design process, underrelaxation is necessary to guarantee the calculation convergence especially during the first few iterations because the calculated perturbation might be deformed as a result of too large pressure differences near the leading edge while the overrelaxation should generally be used for accelerating the convergence speed. But the relaxation factor cannot be made constant directly because 1) the geometric perturbations near leading edge tend to be larger owing to large pressure gradients and they oscillate and contain some noises; 2) geometric perturbations are too large in the supersonic region of transonic flows as the flows are very sensitive to smaller perturbations; and 3) geometric perturbations are generally smaller in the aft part of airfoil upper surface and on the lower surface at large angles of attack. This might be caused by taking the same constant D in Eqs. (17) and (26) for the entire airfoil. The problem can be solved by treating the constant D as a function of curvature lengths, but it is more convenient to use nonuniform relaxation. Therefore in this research, different relaxation factors are employed and varied between 0.3 and 5 in Eqs. (17) and (26), and are adjusted automatically according to the amplitudes of geometric perturbations and the pressure differences. Relaxation factors should be selected in such a way that the convergence speed to the target values should be more uniform at every point of the airfoil. If the pressure differences in one part of the airfoil are already near zero and there are still larger differences in the other part, the convergence is much slower. In addition, a large relaxation factor can sometimes give rise to a serious problem that small perturbation waves are amplified. The amplified waves reduce the convergence speed rather than accelerate it, which is one of reasons why geometry smoothing is necessary.

Airfoil Design Results

Airfoil Design for High Subsonic Flows

To avoid complicated flows containing shock waves, the first test design is selected for $M_\infty = 0.6$, $Re = 1.0 \times 10^7$, and $\alpha = 1.5$ deg. The target airfoil is RAE 2822, and the initial airfoil is NACA 0012. The large difference between the two airfoils is suitable for testing the capability of the method. The strained coordinate transfer is used during the first 10 iterations. The strained points are the leading edge, the trailing edge, the pressure peak location and the stagnation point during the first five iterations, whereas in the next five iterations the same strained points are selected except the pressure peak location.

The design results are presented in Figs. 4a and 4b to show the pressure distribution and the airfoil shape comparisons between the initial, target, and design airfoils. The convergence is very fast, the differences between the target and design are small even after five design iterations, for example, and the lift coefficient difference is smaller than 1%, which is appropriate for initial design problems. After 15 iterations, the pressure differences are very small, the maximum pressure coefficient difference, which appears near the leading edge, is 0.006, whereas the geometric difference is smaller than

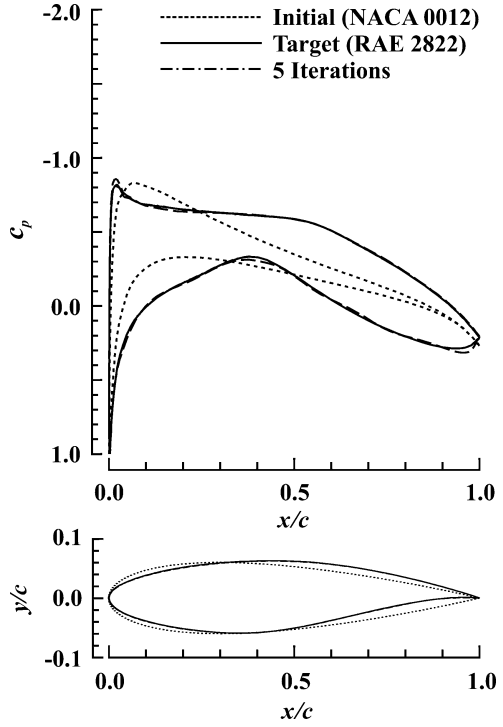

Fig. 4a Inverse airfoil design results: comparison of airfoil geometry and pressure distributions for $M_\infty = 0.6$, $Re = 1.0 \times 10^7$, and $\alpha = 1.5$ deg after five iterations.

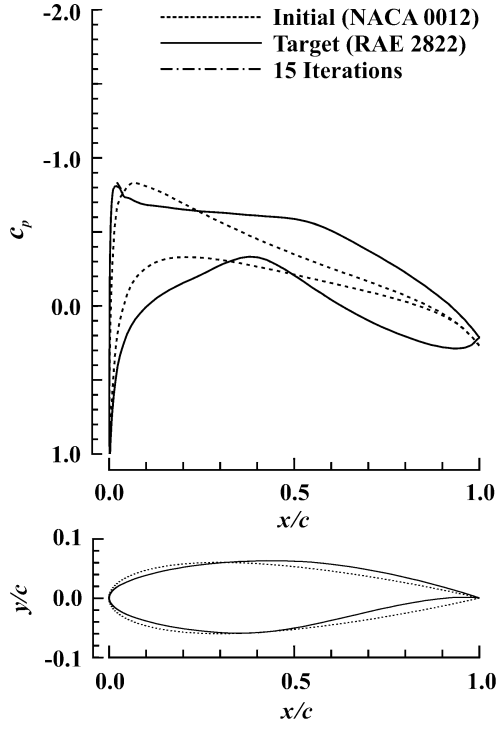

Fig. 4b Inverse airfoil design results: comparison of airfoil geometry and pressure distributions for $M_\infty = 0.6$, $Re = 1.0 \times 10^7$, and $\alpha = 1.5$ deg after 15 iterations.

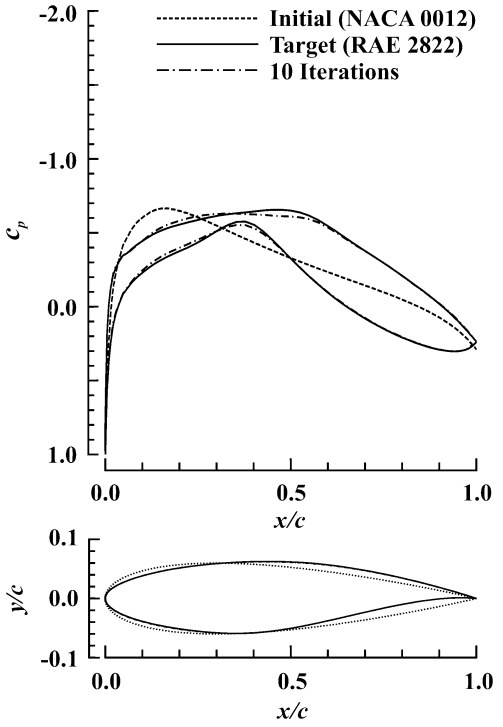

Fig. 5a Inverse airfoil design results: comparison of airfoil geometry and pressure distributions for $M_\infty = 0.725$, $Re = 1.0 \times 10^7$, and $\alpha = 0.0$ deg after 10 iterations.

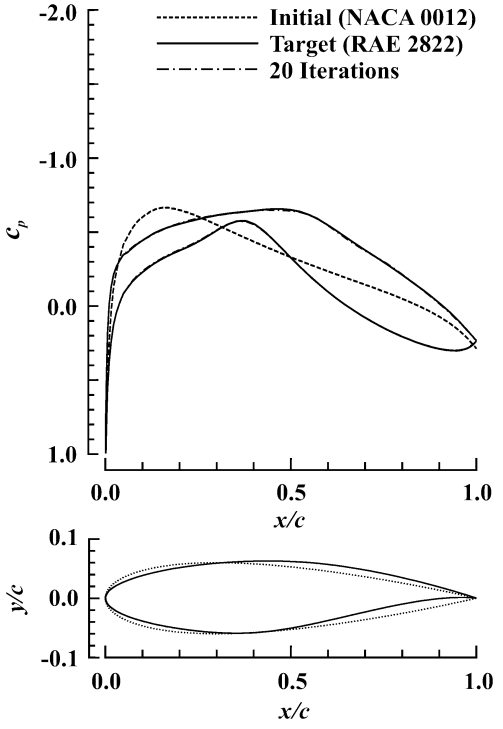

Fig. 5b Inverse airfoil design results: comparison of airfoil geometry and pressure distributions for $M_\infty = 0.725$, $Re = 1.0 \times 10^7$, and $\alpha = 0.0$ deg after 20 iterations.

5.0×10^{-5} considering the tolerance used in aerodynamic design. The precision is surprisingly good.

Another design case, shown in Figs. 5a and 5b, is for $M_\infty = 0.725$, $Re = 1.0 \times 10^7$, and $\alpha = 0.0$ deg. The target and the initial airfoils are again RAE 2822 and NACA 0012, respectively. But the strained coordinate transfer is not applied because of the larger differences of the suction peak locations between the target and the initial pressure distributions. In addition, the stagnation point locations are too close to the leading edge to be calculated with enough accuracy just from the pressure distributions at given x locations.

The convergence is not as good as in the previous case because a supersonic region appears on the upper surface of the initial airfoil during the first few iterations and the strained transfer is not used. But it is still fast enough. In 20 design iterations the pressure coefficient differences are smaller than 0.0045 in the leading-edge region and 0.007 in the remaining part.

Airfoil Design for Low-Speed Flows

The design case is selected for $M_\infty = 0.3$, $Re = 1.0 \times 10^7$, and $\alpha = 4.0$ deg. The target airfoil is RAE 5212, and the initial airfoil is NACA 0012. The strained transfer is used during the first 10 iterations. From the results, as illustrated in Figs. 6a and 6b, the convergence is very fast. In five iterations, the geometry and pressure differences between the target and design are small, and the lift coefficient difference is smaller than 3%. In 15 iterations, there is no discernable difference between the pressure distributions. Moreover, the lift coefficient difference is smaller than 0.001.

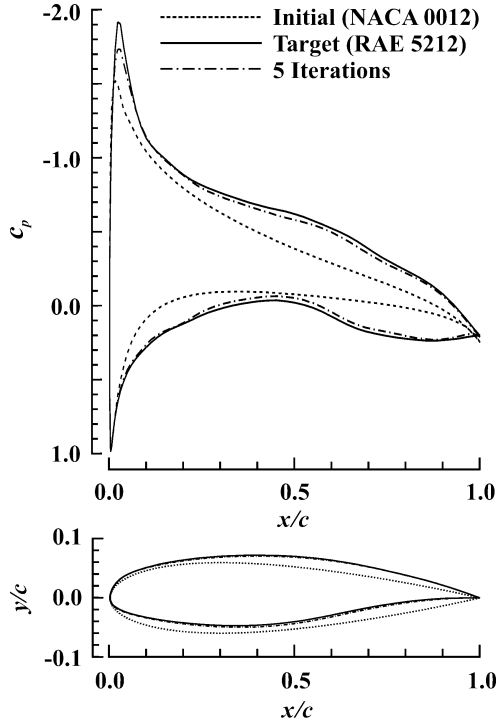

Fig. 6a Inverse airfoil design results: comparison of airfoil geometry and pressure distributions for $M_\infty = 0.3$, $Re = 1.0 \times 10^7$, and $\alpha = 4.0$ deg after five iterations.

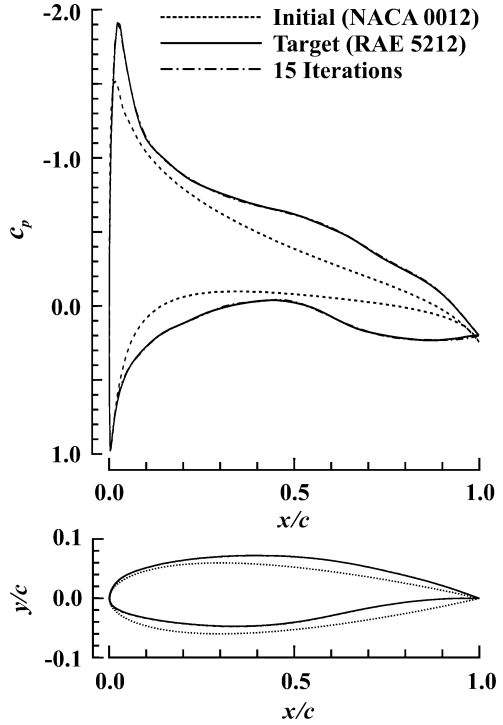

Fig. 6b Inverse airfoil design results: comparison of airfoil geometry and pressure distributions for $M_\infty = 0.3$, $Re = 1.0 \times 10^7$, and $\alpha = 4.0$ deg after 15 iterations.

Transonic Airfoil Design

The design conditions are $M_\infty = 0.715$, $Re = 1.0 \times 10^7$, and $\alpha = 2.30$ deg. The target airfoil is RAE 2822, and the initial airfoil is NACA 0012. The strained transfer is used for the first 20 iterations. The results are presented in Figs. 7a–7c. The convergence is fast. In five design iterations, the geometric differences, as shown in Fig. 7a, between the target airfoil and the design are small, but the pressure

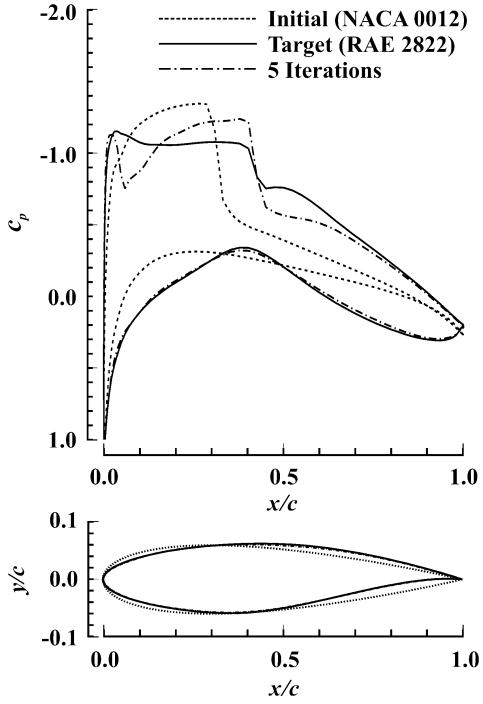

Fig. 7a Inverse airfoil design results: comparison of airfoil geometry and pressure distributions for $M_\infty = 0.715$, $Re = 1.0 \times 10^7$, and $\alpha = 2.30$ deg after five iterations.

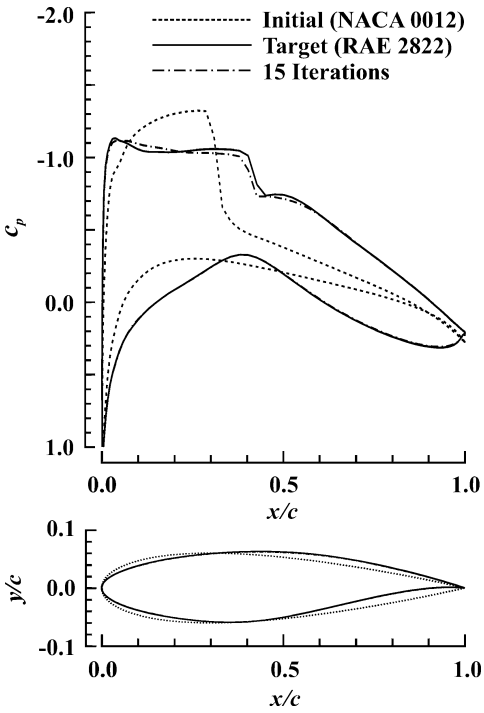

Fig. 7b Inverse airfoil design results: comparison of airfoil geometry and pressure distributions for $M_\infty = 0.715$, $Re = 1.0 \times 10^7$, and $\alpha = 2.30$ deg after 15 iterations.

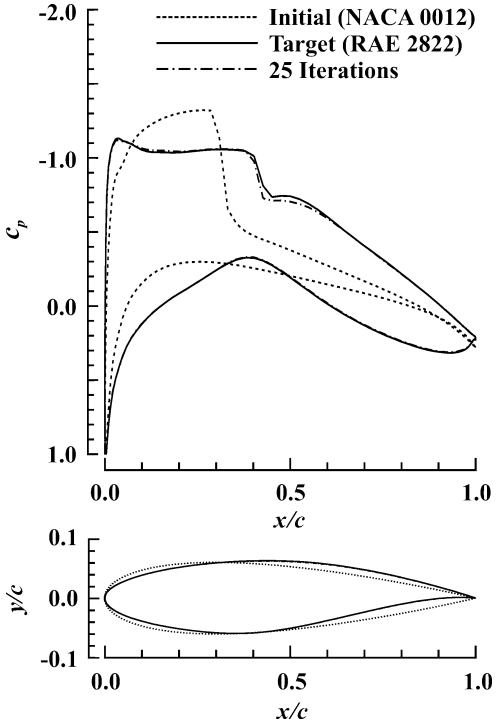

Fig. 7c Inverse airfoil design results: comparison of airfoil geometry and pressure distributions for $M_\infty = 0.715$, $Re = 1.0 \times 10^7$, and $\alpha = 2.30$ deg after 25 iterations.

distribution differences are still large owing to the sensitivity of transonic flows to small perturbations. From the pressure distribution of the design airfoil, two shocks appear during the first few design iterations, which make the flow complicated and the convergence much slower. The first shock is caused by the invisible variations of the curvature in this region. It is possible to solve this problem by smoothing appropriately.

The comparison results, shown in Fig. 7b, in 15 design iterations demonstrate that the pressure distribution of the design airfoil is aerodynamically favorable, the lift coefficient difference between the target and the design is smaller than 2%, and the shock strength is little less than that of the target. From the comparison results, shown in Fig. 7c, after 25 design iterations, the pressure distribution of the design airfoil around the suction peak coincides with that of the target (a difference of less than 0.005), which indicates that the calculation for the leading-edge region is accurate. The results are satisfactory from a practical point of view and from comparisons with the transonic results[1,3–5] of the other iterative methods. However, there are visible pressure differences near the shock locations, which are probably caused by the following factors. As a pressure jump appears owing to the shock wave at the same location, there is also a jump in calculated geometric perturbations. Furthermore, the calculated geometric perturbations are greatly deformed near the shock locations of the target and design airfoils. Smoothing is generally used for solving this problem. But it is hard to make the two shocks coincide together because it is very difficult to accurately control the smoothing effects.

Conclusions

The following conclusion can be drawn from this research:

1) The new method is not only very efficient but also accurate enough for both compressible and low-speed flows, especially the leading-edge shape can be precisely calculated, which compensates for the deficiencies of the many other methods.

2) The efficiency and the accuracy of the method depend greatly on the techniques such as the strained coordinate transfer, geometry smoothing, and nonuniform relaxation for accelerating the convergence. A detailed study and understanding of these techniques can further help improve the efficiency and accuracy of the method.

3) The transonic correction based on the assumption for the effects of waves reflected from the free boundary (sonic line) is effective, but detailed studies regarding its potential to improve transonic solutions should be conducted.

4) A fully automated strained coordinate transfer is an effective way to accelerate the convergence, but further research on its ability to accurately reflect the geometric variations should be made.

For the treatment of geometric discontinuity caused by shock waves, new techniques must be explored to replace the commonly used techniques such as airfoil smoothing in order to meet higher precision requirements in transonic flows.

Acknowledgments

This research was supported by the Natural Sciences and Engineering Research Council of Canada (NSERC) under Grant #1506, which is greatly appreciated. The authors are also grateful to King Fahd University of Petroleum and Minerals, Dhahran, Saudi Arabia, for its support in accomplishing this study. The authors would like to express their gratitude to Mark Drela of Massachusetts Institute of Technology for the use of his MSES code. Last but not the least, the authors are also very grateful to Fassi Kafyeke and his team at Advanced Aerodynamics Department, Bombardier Aerospace, for their support and helpful discussions.

References

[1]Takanashi, S., "Iterative Three-Dimensional Transonic Wing Design Using Integral Equations," *Journal of Aircraft*, Vol. 22, No. 8, 1985, pp. 823–829.

[2]Milholen, William, E., II, "Efficient Inverse Aerodynamic Design Method for Subsonic Flows," *Journal of Aircraft*, Vol. 38, No. 5, 2001, pp. 918–923.

[3]Campbell, R. L., "Efficient Viscous Design of Realistic Aircraft Configurations," AIAA Paper 98-2539, June 1998.

[4]Yu, N. J., and Campbell, R. L., "Transonic Airfoil and Wing Design Using Navier-Stokes Codes," AIAA Paper 96-2651, June 1992.

[5]Barger, R. L., and Brooks, C. W., Jr., "A Streamline Curvature Method for Design of Supercritical and Subcritical Airfoils," NASA TN D-7770, Sept. 1974.

[6]Bernard, E., Schmitz, A., Boscher, E., Garcia, N., and Cebeci, T., "Two-Dimensional Aircraft High-Lift System Design and Optimization," AIAA Paper 98-0123, Jan. 1998.

[7]Hartwich, P. M., and Agrawal, S., "Orthonormal Functions for Airfoil and Wing Parameterization," *Proceedings of the 14th Applied Aerodynamics Conference*, AIAA, Reston, VA, 1996, pp. 359–369; also AIAA Paper 96-2419.

[8]Ferrari, C., and Tricomi, F. G., *Transonic Aerodynamics*, John Hopkins Univ., Silver Spring, MD, 1968.

[9]Moulden, T. H., *Fundamentals of Transonic Flow*, Wiley-Interscience, New York, 1984.

[10]Drela, M., "Transonic Low-Reynolds Number Airfoils," *Journal of Aircraft*, Vol. 29, No. 6, 1992, pp. 1106–1113.

[11]Drela, M., and Giles, M. B., "Viscous-Inviscid Analysis of Transonic and Low Reynolds Number Airfoils," *AIAA Journal*, Vol. 25, No. 10, 1987, pp. 1347–1355.

[12]Giles, M. B., and Drela, M., "Two-Dimensional Transonic Aerodynamic Design Method," *AIAA Journal*, Vol. 25, No. 9, 1987, pp. 1199–1206.

[13]Lighthill, M. J., "A Technique for Rendering Approximate Solutions to Physical Problem Uniformly Valid," *Philosophy Magazine*, Vol. 40, 1949, pp. 1197–1201.

[14]Stahara, S. S., "Rapid Approximate Determination of Nonlinear Solutions: Application to Aerodynamic Flows and Design/Optimization Problems," *Transonic Aerodynamics, Progress in Astronautics and Aeronautics*, edited by David Nixon, Vol. 81, 1984, p. 637.

[15]Nixon, D., "Perturbation of a Discontinuous Transonic Flows," *AIAA Journal*, Vol. 16, No. 1, 1978, pp. 47–52.

[16]Nixon, D., "Perturbation in Two and Three-Dimensional Transonic Flows," *AIAA Journal*, Vol. 16, No. 7, 1978, pp. 699–709.

[17]Yu, J., Saeed, F., and Paraschivoiu, I., "An Iterative Inverse Design Method Based on Aerodynamic Streamline Equations," AIAA Paper 2003-0214, Jan. 2003.

[18]Yu, J., Saeed, F., and Paraschivoiu, I., "Efficient Optimized Airfoil Parameterization," AIAA Paper 2003-0725, Jan. 2003.

[19]Yu, J., "New Efficient Methods for Airfoil Parameterization and Iterative Inverse Aerodynamic Design," M.S. Thesis, Dept. de Genie Mecanique, Ecole Polytechnique de Montreal, Univ. of Montreal, Canada, May 2002.

[20]Renz, W., "Interactive Smoothing of Digitized Point Data," *Computer Aided Design*, Vol. 14, No. 5, 1982, pp. 267–269.